Noniterative Exact Solution to the Phase Problem in Optical Imaging Implemented with Scanning Probe Microscopy

Danielle R. Honigstein,[†,‡] Jacques Weinroth,[†,‡] Michael Werman,[‡] and Aaron Lewis[†,‡,*]

[†]Department of Applied Physics and [‡]Selim & Rachel Benin School of Engineering & Computer Science, Hebrew University of Jerusalem, Israel

Phase retrieval has long been an issue in fields ranging from microscopy to astronomy. Many algorithms have been implemented to retrieve phase,[1−6] but all of the algorithms are iterative and subject to problems of iterative algorithms such as non-convergence, slow convergence, convergence to local minima, and stagnation.[5,7,8] Also, they depend on external parameters to control convergence and noise damping, some of which are empirical and others can be calculated to upper or lower bounds.

In X-ray crystallography, phase retrieval has classically used a methodology of isomorphous replacement in which a heavy atom is introduced as a reference signal. Diffraction patterns are obtained with and without the presence of the heavy atom, and from this difference, the phase is retrieved.[9]

An atomic force controlled point source of light used in near-field scanning optical microscopy (NSOM) can act as a point source propagating into the far-field with a detectable intensity. It is in fact a delta function or an optical "heavy atom" that can with nanometric precision be positioned freely on or relative to a sample. Thus, the intensities of light from an object can be recorded at the Fourier plane with and without the presence of this optical delta function as it has been possible in X-ray crystallographic phase retrieval with the addition of heavy atoms. Table 1 compares the terms used in crystallography to those used in the HARPS method described in this paper.

No paper has addressed such a combination of technologies to resolve the phase problem, but about 20 years ago, an algorithm based on the use of heavy atom concepts was proposed in optics by Kim and Hayes.[10] This algorithm restores phase using Fourier intensity images of a sample

ABSTRACT An object is characterized by its amplitude and phase. However, when acquiring optical data about such an object, using a recording medium such as a camera, phase information is lost. Crystallography experienced a breakthrough in phase retrieval for large molecular entities by Max Perutz's introduction of "heavy atoms" using the method of isomorphous replacement. The availability of scanning probe microscopy and its full integration with optical microscopy allows us to apply these X-ray concepts to implement "heavy atom" restoration of phase in optical phase retrieval. In analogy to the heavy atom method, we acquire Fourier intensities in place of an X-ray diffraction pattern, and in place of the heavy atom, we utilize a nanometrically translatable point source of light based on the propagating field of a cantilevered near-field scanning optical microscopic (NSOM) probe controlled by an atomic force microscope (AFM). This integration of NSOM/AFM technology with far-field imaging achieves robust phase retrieval independent of external parameters, leading to 3D optical imaging. The methodology has super-resolution potential, and thus, heavy atom restoration of phase with super-resolution (HARPS) shows the potential of transparently integrated scanning probe microscopy with optical and other imaging modalities such as electron or ion optical imaging.
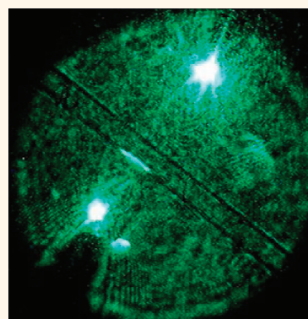
KEYWORDS: phase retrieval · phase ambiguity · X-ray heavy atom · noniterative · NSOM · optical · AFM · HARPS · multiprobe · super-resolution · inverse problem

and a reference signal. The algorithm was presented without any simulation and without any relation to optical microscopy but was presented as a general methodology in optics. The present paper realizes the application of this algorithm to real problems in conventional optical microscopic imaging. The result is a solution which directly solves for the optical phase with no external parameters, such as those used in iterative algorithms, to ensure convergence and smoothing of the noise.

Our paper implements this algorithm to optical microscopy using a nanometric point

source of light as the heavy atom and using the optical Fourier transform in place of the data that are obtained in X-ray diffraction. This results, without iteration, in height measurements similar to AFM height data of a sample but in parallel and, thus, at a fraction of the time that it would have taken to record such an AFM image.

RESULTS AND DISCUSSION

The motivation for this work was to ascertain the feasibility of applying crystallographic heavy atom methodology for optical imaging. Using the Kim and Hayes paper, we "translate" the crystallographic terms into implementable optical elements. The light emanating from a tapered cantilevered optical fiber is applied as a nanometric source of light, analogous to a heavy atom, while the optical Fourier transform of the object is employed in analogy to the X-ray diffraction data. In crystallography, the algorithm used gives very precise results as a result of a refinement procedure which historically involved the use of two heavy atoms. In this first demonstration of the application of these concepts to optics, no such refinement with two heavy atoms has been attempted.

For these initial investigations with HARPS, two samples were studied, first, defined grooves in a photoresist and, second, erythrocyte cells. Both results can be seen in Figure 1. From the results on the grooves, the average phase difference between the imaged grooves and the background was 4.4 radians (with up to 5% error). Equation 1 was used to calculate the pattern depth:

$$\Delta H = \frac{\lambda \times \Delta \varphi}{2\pi \Delta n} \qquad (1)$$

where λ is the wavelength of the laser, $\Delta \varphi$ is the phase difference calculated from the experiment, and $\Delta n = n_{sample} - n_{air} = 0.6496$. The corresponding depth of the sample resulting from the algorithm and averaging over the length of the line was 573 nm, in accordance with the average AFM result of 574 nm.

Line scans show that the sharpness of the restored image is 0.57 μm (measured between 30 and 70% of the step). The AFM sharpness was 0.26 μm ($\sim$50%). The objective used was 100$\times$ with a numerical aperture of 0.8, which, together with the 532 nm laser illumination wavelength, would have predicted a resolution of 0.40 μm according to the Rayleigh criterion. By using super-resolution techniques and refinement methods in analogy to the heavy atom method, we hope to implement in the future super-resolution with such optical heavy atom methodology.

To generalize our results, the same algorithm was applied to a sample of red blood cells in a drop of fresh blood. In Figure 1b, the typical biconcave structure of a red blood cell is seen. The size of the red blood cell was 7 μm, and from the phase restoration, the concave center was 275 nm deep. To obtain this result, the refractive index of blood was taken to be 1.4[11] and compared with air. The depth is in accordance with Wu et al.,[12] especially considering that the blood was not treated or fixed and had commenced to dry.

It is worthwhile to compare optical imaging with HARPS to conventional optical imaging. When imaging with monochromatic light, the image is a linear mapping of the complex amplitude. When imaging with non-monochromatic light, the image is a linear mapping of the intensity.[13] In HARPS, we get both the complex amplitude and the phase. Optic images with monochromatic and non-monochromatic light are shown in Figure 2.

TABLE 1. Parallelism of Terms

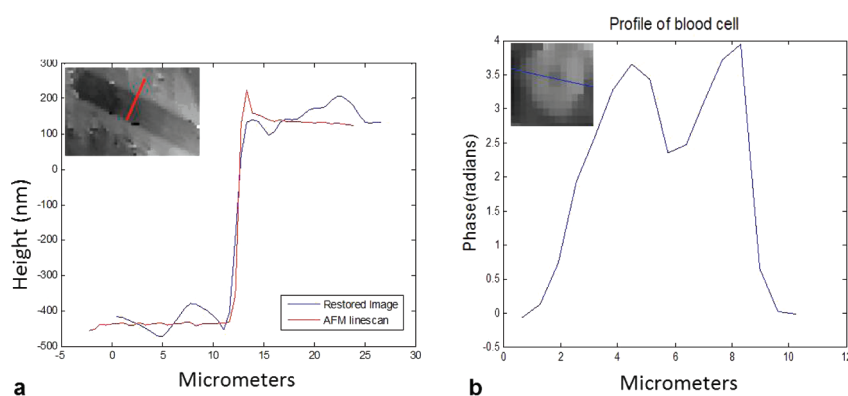| crystallography	HARPS
heavy atom	NSOM tip
X-ray diffraction	optical Fourier transform
Patterson function	difference autocorrelation

Figure 1. (a) Comparison of AFM line scan and profile along red lines on the restored phase image [inset] using heavy atom restoration of phase with super-resolution (HARPS). Inset: Restored photoresist sample with rectangular structures with 560-610 nm grooves. (b) Restored erythrocyte cell [inset], with blue line showing location of profile which replicates well what is obtained with AFM. Inset: Restored phase image of erythrocyte cell.
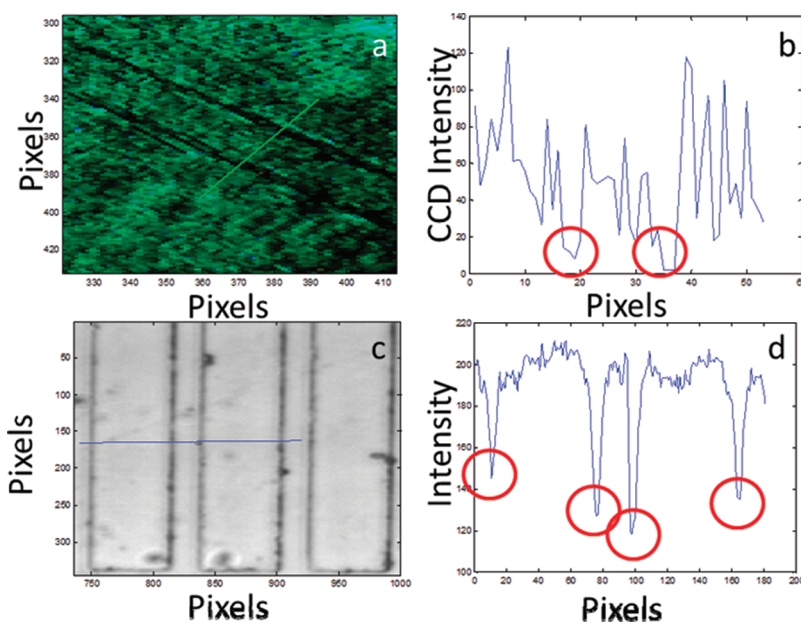
Figure 2. (a) Monochromatic light image of the photoresist sample. **(b)** Profile on green line of image a. **(c)** Non-monochromatic light image of calibration sample with constant amplitude. **(d)** Profile on blue line of (c). Red circles mark the edges.

Optic images tend to emphasize the edges of the image and give no data as to the relative height or other data of the features in the image. This is especially true in transparent samples such as the ones shown.

When comparing HARPS to other quantitative phase restoration methods such as employed by Axelrod *et al.*[14] using DIC, we can see that HARPS has obvious advantages over these methods: There are no built-in artifacts such as ringing (typically caused by the iterative algorithms used), fringes (caused by the shear vector in DIC), and halos (typical of phase contrast microscopy methods). The main problem with the current version of HARPS is noise, and that can easily be ameliorated with future design improvements.

CONCLUSIONS AND PROSPECTS

In conclusion, we have presented a direct and exact method of retrieving phase in optical imaging. It requires no iteration, no external parameters, and no approximations. This wide-field ability to rapidly and in parallel optically image the phase of objects or collections of objects has considerable general applicability. This extends from biology to quality control in the assembly of optical and other components.

Although the present instrumentation can be considerably improved (better alignment mechanisms, a better CCD with saturation prevention, upright microscope imaging, automation for video rate phase imaging, *etc.*), it is already evident that the approach lends itself to obtaining super-resolution in optical imaging in *X*, *Y*, and *Z*.

As is well-known, the basis for obtaining super-resolution is multiple images.[20] This of course can be obtained in a cumbersome way by moving the sample, which would require the accurate verification of the exact sample movement. This could be done in our method by the presence of an online AFM. However, as shown in the Methods section, a single nanometrically exact and known subpixel movement of the tip with its reference signal automatically results in the restored image shifting without any sample movement. This would predict that, even without using any of the constraint-based approaches that are critical for refinement of the structure in X-ray crystallography, one should be able to obtain, using simply standard super-resolution multiple image algorithms,[20] a resolution of 200 nm. In addition, using the speckles of the laser can also improve the resolution.[21]

Furthermore, in the same vein of emulating the heavy atom approach of X-ray crystallography, the method of multiple heavy atoms, which we know is critical for structure refinement in X-ray crystallography, can be emulated in optics with two or more optical heavy atoms using presently available multiprobe AFM/NSOM techniques. Such emulation should be experimentally even less complex than in X-ray crystallography since there is no chemical modification barrier in our optical approach as is the case of implementing multiple heavy atoms at different sites in X-ray diffraction with amplitude but no phase changes. To apply multiple optical heavy atoms, the new approach of multiprobe NSOM[16] can be used or single probes with the reference signals positioned at different nanometrically defined locations can be used.

In both of these approaches, there will be a refinement of the results as in multiple heavy atom constrained-based refinements in X-ray-based image reconstruction.

Besides super-resolution, the methodology could have an impact on fundamental optics by, as mentioned above, using single or multiple probe tips with a known difference in height to either significantly simplify or resolve the unsolved problem of phase unwrapping.

One also has to consider the application of this methodology to other imaging modalities. An example where the method could have significant import is in phase imaging with electron microscopy. This is specifically relevant since there is a growing movement to put an AFM in electron and ion beams[22] and one could conceive of the tip of an AFM with an electron-rich material translated by AFM as in the optical heavy atom analogy.

A more challenging direction will be to image "slices" of a thick sample and piece them together to perform 3D phase imaging. Sample tilting approaches have revolutionized such 3D reconstructions in electron and optical microscopy, and some of the approaches could well be employed to help solve/resolve some of the complexity that is expected in 3D slicing and reconstruction. In such extensions, it is anticipated that the ability to nanometrically move the tip in Z and experimentally unravel the phase unwrapping issues should be of significant import.

In summary, this paper provides a direct solution to the phase problem in imaging with definitive approaches for super-resolution. This new method has been applied successfully to two imaging tasks in this paper, and from the results already obtained, it is clear that the method can be applied widely to phase restoration. Thus, one could potentially address problems in cell biology that are associated with cellular mechanics that today are preferentially measured with the very slow technique of AFM. An example is the metastatic potential of cells from cancer patients.[23] In addition, within such a biological medical theme, one could even consider the methodology for rapid parallel acquisition of data similar to optical coherence tomography and using it for the measurement of phase changes in tissues.

Thus, the prospects for this method seem quite bright for a number of different phase imaging tasks where speed, phase, and even super-resolution are essential.

Finally, a most important aspect of this paper is the criticality of online scanned probe microscopy to address problems in imaging by providing data that have not been accessible in the past for addressing the inverse problem that is imaging.

METHODS

To explore the Kim and Hayes algorithm, we prepared lithographic grooves on an AZ1500 series photoresist (AZ Electronic Materials, Inc.) for which the index of refraction was known. The resulting sample could readily be analyzed by atomic force microscopy (AFM). The grooves had a varying depth of 560−610 nm, with an average of ~574 nm. The refractive index was 1.63496 at 532 nm, the illumination wavelength. In addition, we have also imaged erythrocyte cells in a drop of blood placed on a slide.

For this development in optical imaging, an inverted microscope and a Fourier system (an f−f configuration) were employed to acquire the Fourier transform of the enlarged sample. The system configuration is similar to that used by Popescu et al. in Fourier phase microscopy.[15] For technical reasons, we used transparent samples even though the algorithm and the experimental arrangement that we have devised is fully applicable to image reflecting samples in an upright microscope setting.

Light emitted from a single longitudinal mode 30 mW Nd:Yag (frequency doubled) laser (MSL-III-532, long coherence length, Changchun New Industries, Changchun, China) is divided by a beam splitter into two beams, as shown in Figure 3. One beam is coupled to a single mode fiber, and the light emerging at the other end of this fiber is collimated in order to obtain a plane wave. The single mode fiber also acts as a spatial filter. The other beam is coupled into a multimode optic fiber culminating in an NSOM tip attached to a MultiView 4000 scanned probe microscope (Nanonics Imaging Ltd., Jerusalem, Israel) fully integrated into a Zeiss Axiovert 135 inverted optical microscope.

The virtual image plane (VIP) is the plane of the enlarged sample image, illuminated by a virtual point source. By placing a lens at the VIP, the virtual point source is transformed to a virtual plane source, and the standard f−f configuration is placed after the VIP to get the Fourier intensity images at the CCD (Figure 3).

The CCD used was a DT4000 uncooled camera from DuncanTech-Redlake (Florida, USA).

The tip used in the experiments reported in this paper had a 300 nm diameter. The tip was brought into contact with the sample using AFM feedback. With the probe tip maintained with AFM in contact with the sample three images were taken: (1) with light propagating through the NSOM tip, (2) without light in the NSOM tip, and (3) with light only through the NSOM tip. An example of (1) with two tips is shown in the Table of Contents graphic.

The phase was restored using the Kim and Hayes algorithm, which is qualitatively described in Figure 4. Let x represent the sample, h the reference, and $y = x + h$ is both together (see Figure 4). Let also $X = $ Fourier(x), $Y = $ Fourier(y), $H = $ Fourier(h) (not shown). The measured data is $F = |X|^2$, the Fourier intensity of the sample; $G = |Y|^2$, the Fourier intensity of the sample and reference; and $R = |H|^2$, the Fourier intensity of the reference signal (Kim and Hayes assume that R is known a priori, and in our implementation, R is measured). From F, G, and R can be obtained the autocorrelation of x, h, and y via an inverse Fourier transform, denoted Rx, Rh, and Ry, respectively. The "difference autocorrelation" is $Ryxh = Ry - Rx - Rh$. If h is a delta function, then $h = A\delta(m_0, n_0)$ and then $Ryxh$ becomes

$$Ryxh(m, n) = Ax*(m_0 - m, n_0 - n) + Ax(m_0 + m, n_0 + n) \quad (2)$$

where $x*$ denotes the complex conjugate of x.

The relationship between the difference autocorrelation and x, y, and h is illustrated in Figure 4. The difference autocorrelation, $Ryxh$, shows x, the sample, twice, slightly overlapped. One of the samples is conjugated and rotated by 180° relative to the other. Each element in the right side of eq 2 refers to one of the samples in $Ryxh$. The position of the reference delta (the point light source) determines the amount and location of the overlap
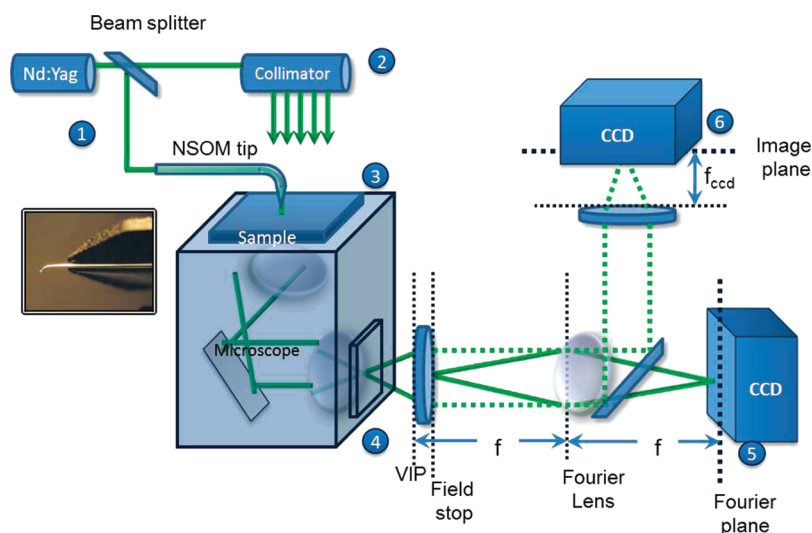
Figure 3. System includes the following: (1) Nd:Yag laser beam is split and coupled to two fibers. (2) Part of the light is collimated in order to illuminate the sample 3. The other light path is coupled to an NSOM tip, brought into contact with the sample by means of an AFM control system. (4) Collimated virtual image plane (VIP). (5) Fourier plane, using the f−f configuration. (6) Image plane. Inset: NSOM tip.
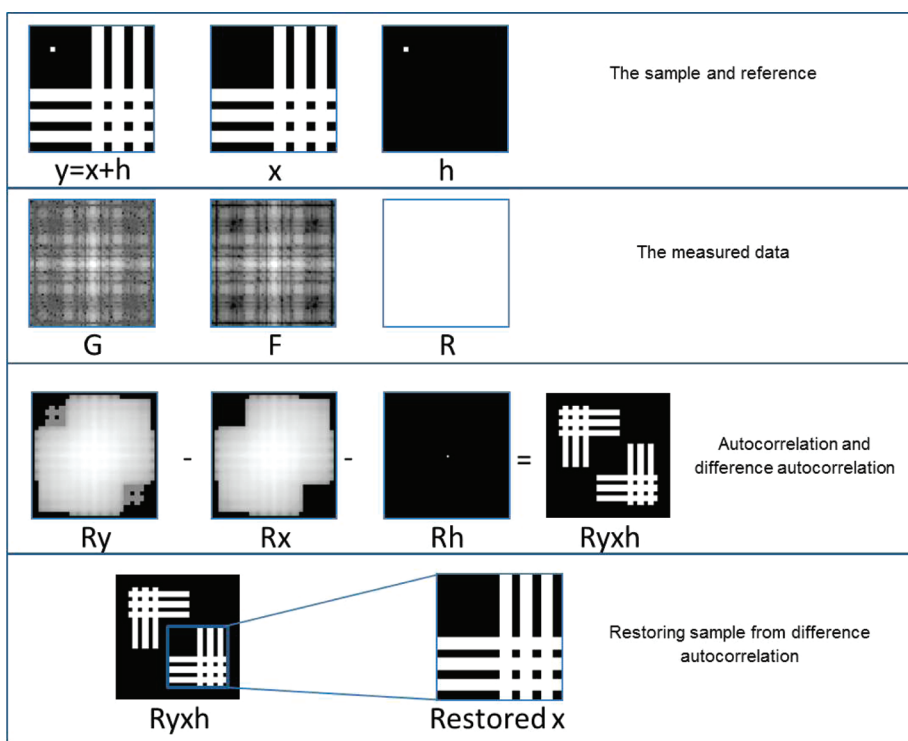

Figure 4. Illustration of the restoration algorithm. Fourier magnitude is shown in log scale.

(see Figure 5). The difference autocorrelation is a complex image that includes the phase of x. In addition, the position of the tip can be used to move the restored phase images relative to each other by subpixel amounts, providing an opportunity for super-resolution in addition to phase restoration.

If the reference delta is located on the edge of the field of view of the sample and outside the area of interest, the area of interest in x can be copied directly from the difference autocorrelation. If the area of interest in the sample is in the overlap area, the overlapping part needs to be separated. It is separated using the measured image G (which is a Fourier transform of the sample autocorrelation) using an iterative

procedure. This iterative procedure was analyzed with simulations and experimental data and has proved to be extremely sensitive to noise as it accumulates such noise from former iterations.

For the data presented in this paper, the reference delta was placed outside of the area of interest and therefore the above problem was circumvented. However, for a more general solution, two reference delta functions can be used. This can be accomplished using developments in multiprobe NSOM techniques, shown in the Table of Contents graphic.[16] Our ability to implement this solution is shown in Figure 6 using a dual probe MV4000 system integrated with the optical microscope
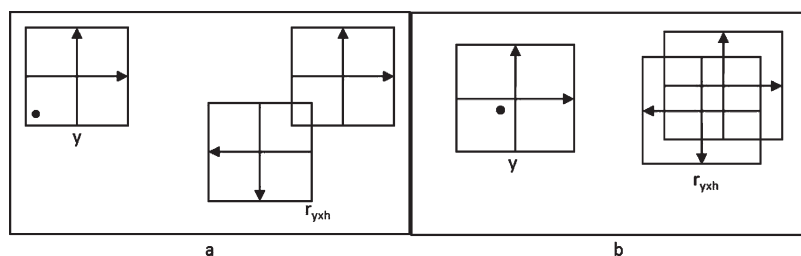
Figure 5. Relation between reference function position and overlap in *Ryxh*. (a) Reference position at the edge of field of view. (b) Reference position at the center of field of view.
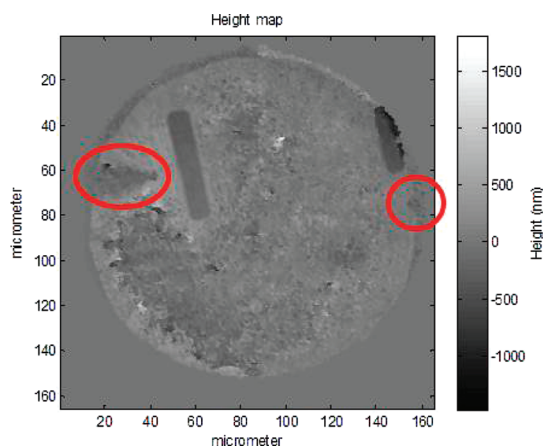

Figure 6. Restoration based on dual multiprobe AFM/NSOM system. In the restored image, both the trench in the photoresist and the two NSOM probes are restored. The left-hand tip was restored by the presence of the right tip and *vice versa*.

(Nanonics Imaging Ltd., Jerusalem, Israel). In this figure, the photoresist is restored, and in addition to the trench in the photoresist, the two NSOM tips are clearly seen in the restoration. In the future, this technique of AFM-controlled multiple probe tips with a known difference in height could be utilized to simplify phase unwrapping. In the present paper, however, we used existing methods[17−19] (see Figure 1a). In pixels where the amplitude is extremely low, the phase is not well-defined and jumps randomly between $-\pi$ and π. Therefore, in all pixels where the amplitude was less than 0.05% of the maximum value, we "damped" the phase value by dividing it by 2.

In the examples shown in this paper, the total measurement time was at most 5 s (depending on the acquisition rate of the camera when taking three images) and the computing time was 3−4 s. All processing was done on a computer with Windows 7, 64 bit operating system, with a quad core Intel Core i7 CPU at 2.93 GHz.

REFERENCES AND NOTES

1. Marchesini, S.; He, H.; Chapman, H. N.; Hau-Riege, S. P.; Noy, A.; Howells, M. R.; Weierstall, U.; Spence, J. C. H. X-ray Image Reconstruction from a Diffraction Pattern Alone. *Phys. Rev. B* **2003**, *68*, 140101(R).

2. Pfeiffer, F.; Weitkamp, T.; Bunk, O; David, C. Phase Retrieval and Differential Phase-Contrast Imaging with Low-Brilliance X-ray Sources. *Nat. Phys.* **2006**, *2*, 258–261.

3. Nugent, K. A.; Paganin, D.; Gureyev, T. E. A Phase Odyssey. *Phys. Today* **2001**, *54*, 27–32.

4. Gerchberg, R. W.; Saxton, W. O. A Practical Algorithm for the Determination of Phase from Image and Diffraction Plane Pictures. *Optik* **1972**, *35*, 227–246.

5. Fienup, J. R. Phase Retrieval Algorithms: A Comparison. *Appl. Opt.* **1982**, *21*, 2758–2769.

6. Schulz, T. J.; Snyder, D. L. Image Recovery from Correlations. *J. Opt. Soc. Am. A* **1992**, *9*, 1266–1272.

7. Fienup, J. R.; Wackerman, C. C. Phase Retrieval Stagnation Problems and Solutions. *J. Opt. Soc. Am. A* **1986**, *3*, 1897–1907.

8. Choi, K; Lanterman, A. D.; Raich, R. Convergence of the Schulz-Snyder Phase Retrieval Algorithm to Local Minima. *J. Opt. Soc. Am. A* **2006**, *23*, 1835–1845.

9. Green, D. W.; Ingram, V. M.; Perutz, M. F. The Structure of Haemogobin IV: Sign Determination by the Isomorphous Replacement Method. *Proc. R. Soc. A* **1954**, *225*, 287–307.

10. Kim, W.; Hayes, M H. Phase Retrieval Using Two Fourier-Transform Intensities. *J. Opt. Soc. Am. A* **1990**, *7*, 441–449.

11. Ghosh, N.; Buddhiwant, P.; Uppal, A.; Majumder, S. K.; Patel, H. S.; Gupta, P. K. Simultaneous Determination of Size and Refractive Index of Red Blood Cells by Light Scattering Measurements. *Appl. Phys. Lett.* **2006**, *88*, 084101.

12. Wu, Y.; Hu, Y.; Cai, J.; Ma, S.; Wang, X.; Chen, Y.; Pan, Y. Time-Dependent Surface Adhesive Force and Morphology of RBC Measured by AFM. *Micron* **2009**, *40*, 359–364.

13. Goodman, J. *Introduction to Fourier Optics*; McGraw-Hill: New York, 1968.

14. Axelrod, N; Radko, A.; Lewis, A.; Ben Yosef, N. Topographic Profiling and Refractive Index Analysis Using Differential Interference Contrast (DIC) with Brightfield Intensity and Atomic Force Imaging. *Appl. Opt.* **2004**, *43*, 2272–2284.

15. Popescu, G.; Deflores, L. P.; Vaughan, J. C. Fourier Phase Microscopy for Investigation of Biological Structures and Dynamics. *Opt. Lett.* **2004**, *29*.

16. Ren, X.; Liu, A.; Zou, C.; Wang, L.; Cai, Y.; Sun, F.; Guo, G.; Guo, G. Interference of Surface Plasmon Polaritons from a "Point" Source. *Appl. Phys. Lett.* **2011**, *98*, 201113.

17. Goldstein, R. M.; Zebken, H. A.; Werner, C. L. Satellite Radar Interferometry: Two Dimensional Phase Unwrapping. *Radio Sci.* **1988**, *23*, 713–720.

18. Spottiswoode, B. 2D Phase Unwrapping Algorithms. Matlab Central File Exchange. [Online] 2008; http://www.mathworks.com/matlabcentral/fileexchange/22504-2d-phase-unwrapping-algorithms.

19. Ghiglia, D. C.; Pritt, M. D. *Two-Dimensional Phase Unwrapping: Theory, Algorithms and Software*; Wiley-Interscience: New York, 1998.

20. Elad, M; Fuer, A. Restoration of Single Super-Resolution Image from Several Blurred, Noisy and Down-Sampled Measured Images. *IEEE Trans. Image Process* **1997**, *6*, 1646–1658.

21. Garcia, J.; Zalevsky, Z; Fixler, D. Synthetic Aperture Super-resolution by Speckle Pattern Projection. *Opt. Express* **2005**, *13*, 6073–6078.

22. Baird, L.; Ang, G. H.; Low, C. H.; Haegel, N. M.; Talin, A. A.; Li, Q.; Wang, G. T. Imaging Minority Carrier Diffusion in GaN Nanowires Using Near Field Optical Microscopy. *Physica B* **2009**, *404*, 4933–4936.

23. Cross, S. E.; Jin, Y. S.; Rao, J.; Gimzewski, J. K. Nanomechanical Analysis of Cells from Cancer Patients. *Nat. Nanotechnol.* **2007**, *2*, 780–783.